Malaysian Journal of Microbiology, Vol 20(4) 2024, pp. 417-429
DOI: http://dx.doi.org/10.21161/mjm.230265

Malaysian Journal of Microbiology
Published by Malaysian Society for Microbiology
(In SCOPUS since 2011)

Sequence, structure and biophysical characterization of CsoR-like hypothetical protein from *Geobacillus zalihae* strain T1

Nasihah Musa[1,2], Ashwaani Mangavelu[1,2], Shaw Xian Au[1,2], Azyyati Mohd Padzil[3], Alexandre Kriznik[4], Muhammad Alif Mohammad Latif[5], Mohd Anuar Jonet[3], Nazahiyah Ahmad Rodzli[3], Thean Chor Leow[1,2], Mohd Shukuri Mohamad Ali[1,6], Raja Noor Zaliha Raja Abd Rahman[1,7], Abu Bakar Salleh[1] and Yahaya M. Normi[1,2]*

[1]Enzyme and Microbial Technology Research Centre, Faculty of Biotechnology and Biomolecular Sciences, Universiti Putra Malaysia, 43400 Serdang, Selangor, Malaysia.
[2]Department of Cell and Molecular Biology, Faculty of Biotechnology and Biomolecular Sciences, Universiti Putra Malaysia, 43400 Serdang, Selangor, Malaysia.
[3]Malaysia Genome and Vaccine Institute, Jalan Bangi, 43000 Kajang, Selangor, Malaysia.
[4]UMR 7365 CNRS-Université de Lorraine, Enzymologie Moléculaire et Structurale, Biopôle, BP 184, 54506 Vandoeuvre-les-Nancy, France.
[5]Center of Foundation Studies for Agricultural Science, Universiti Putra Malaysia, 43400 Serdang, Selangor, Malaysia.
[6]Department of Biochemistry, Faculty of Biotechnology and Biomolecular Sciences, Universiti Putra Malaysia, 43400 Serdang, Selangor, Malaysia.
[7]Department of Microbiology, Faculty of Biotechnology and Biomolecular Sciences, Universiti Putra Malaysia, 43400 Serdang, Selangor, Malaysia.
Email: normi_yahaya@upm.edu.my

Received 25 April 2023; Received in revised form 27 March 2024; Accepted 2 April 2024

ABSTRACT

Aims: To date, nine classes of copper regulation mechanisms have been discovered in bacteria and CsoR regulator protein is the most recent among them. Only a few have been structurally and functionally characterized. The present study was aimed to isolate and characterize the sequence, structure and biochemical properties of $CsoR_{Gz}$-like hypothetical protein (HP) to be potentially used as a copper sensor protein.
Methodology and results: A scan of the complete genome of a *Geobacillus zalihae* strain T1 revealed the presence of CsoR-like ($CsoR_{Gz}$) HP, which contains CsoR-like_DUF156 domain and highly conserved Cys-His-Cys residues essential for copper binding. It only shares moderate sequence identity with structurally characterized CsoR proteins. $CsoR_{Gz}$-like HP was subjected to sequence analyses to identify important domains, motifs and residues, while circular dichroism and X-ray crystallography were used to determine its secondary and tertiary structures. $CsoR_{Gz}$ appears to be a dimer comprising mainly α-helices, with putative, conserved metal-binding ligands, Cys46-His71-Cys75, located on the α2 helix of the protein. Biophysical characterization of $CsoR_{Gz}$ using UV/Vis and fluorescence spectrophotometry confirmed its interaction with Cu(I). Docking of Cu(I) to the dimeric structure of $CsoR_{Gz}$ showed that Cu(I) could be coordinated by the above metal-binding residues, further stabilized by the hydrophobic core at the metal-binding site.
Conclusion, significance and impact of study: The findings in this study suggest that $CsoR_{Gz}$-like HP might be a novel CsoR protein. This adds to the breadth and numbers of possible CsoR proteins, particularly uncharacterized ones, existing in the pool of hypothetical proteins, to be further characterized and compared across bacterial taxa.

Keywords: Biophysical characterization, crystal structure, $CsoR_{Gz}$-like HP, docking, sequence analysis

INTRODUCTION

Copper, as a transition metal, is essentially needed in living things. It plays various roles, such as cofactors for enzymes, which are important in cellular processes (Sakamoto *et al*., 2010; Rademacher and Masepohl, 2012). However, high concentrations of copper will lead to toxicity via the formation of reactive oxygen species (ROS) and interfere with metal-binding by proteins by competing with other metals at the protein binding site (Hiniker *et al*., 2005; Macomber and Imlay, 2009). However, living organisms have metal homeostasis mechanisms in place to overcome such adversities caused by metals. In bacteria, copper regulation, which stabilizes cellular copper concentrations, is an example of such a mechanism. To date, nine classes of copper

***Corresponding author**

ISSN (print): 1823-8262, ISSN (online): 2231-7538

Malays. J. Microbiol. Vol 20(4) 2024, pp. 417-429
DOI: http://dx.doi.org/10.21161/mjm.230265

regulation have been documented and classified based on the organisms in which they have been discovered, namely CueR, CusRS, ComR (in *Escherichia coli*), CopL and CorE proteobacteria in *Xanthomonas* sp. and *Myxococcus xanthus* respectively, BxmR in cyanobacteria and CopY, CsoR, YcnK in Gram-positive bacteria (Rademacher and Masepohl, 2012).

Among these mechanisms, CsoR copper regulation is the most recently discovered mechanism. In this mechanism, CsoR, the copper sensor protein, acts as a regulator (repressor) in the expression of target genes involved in copper homeostasis. The genes include copper chaperone copZ and copper efflux P-type ATPase copA genes (Liu *et al*., 2007; Smaldone and Helmann, 2007). CsoR acts by binding specifically to a promoter region of the copZA operon containing a GC-rich pseudopalindromic sequence (Iwig *et al*., 2006; Ma *et al*., 2009) at low copper (Cu(I)) concentration. In excessive amounts of Cu(I), CsoR binds to the metal ion, thus releasing itself from the regulator-binding site of the copZA operon. This results in the expression of *copZA* genes, which will cause excess Cu(I) to be effluxed from the cell. To date, only a few CsoR proteins are structurally and functionally characterized. This includes CsoR proteins from *Geobacillus thermodenitrificans* Ng80-2, *Thermus thermophilus*, *Mycobacterium tuberculosis* and *Streptomyces lividans* (Liu *et al*., 2007; Sakamoto *et al*., 2010; Dwarakanath *et al*., 2012; Tan *et al*., 2014).

Finding and characterizing more CsoR proteins from other bacterial strains is important for gaining more significant insight and comparisons of this protein across different bacterial taxa. A good platform to find and study such candidates in greater detail would be within the pool of hypothetical proteins (HPs). HPs significantly constitute approximately 30-40% of any given genome (Bork, 2000). They are often referred to as “orphan” proteins due to their unknown functions stemming from their low sequence and structural homology to other known, well-characterized proteins (Roberts, 2004; Hanson *et al*., 2009). In this study, a scan of the genome of a locally isolated *G. zalihae* (Rahman *et al*., 2007) revealed the presence of a sequence encoding CsoR-like hypothetical protein ($CsoR_{Gz}$) containing the conserved, putative Cys-His-Cys metal-binding residues and CsoR-DUF domain with only 30-38% of identity to structurally characterized CsoRs of *G. thermodenitrificans* Ng80-2, *M. tuberculosis* and *S. lividans*. The crystal structure of $CsoR_{Gz}$-like HP was elucidated and compared with other structurally-characterized CsoRs. Docking of Cu(I) to the dimeric structure of the protein and *in vitro* Cu(I) binding assay were carried out to confirm its ability to bind to the metal ion.

MATERIALS AND METHODS

Bacterial strains and plasmids

Geobacillus zalihae was used for genomic DNA extraction to obtain *csoR*$_{Gz}$-like gene. *Escherichia coli* TOP 10 (Invitrogen) was used as the cloning host, while *E. coli* BL21 Star™ (DE3) (Invitrogen) was employed as the expression host for the production of $CsoR_{Gz}$ protein. Plasmid pET-28b(+) (Novagen) was used as the expression vector to express the protein.

$CsoR_{Gz}$ sequence analysis

The sequence of $CsoR_{Gz}$ was obtained from the complete genome of *G. zalihae* and was subjected to BLASTP (Altschul *et al*., 1990) similarity analysis against non-redundant database and Protein Data Bank (PDB) (Berman *et al.*, 2000). ClustalW (Larkin *et al*., 2007) was used for multiple sequence alignment. Domain analyses were performed using the Conserved Domains database (CDD) (Marchler-Bauer and Bryant, 2004), InterPro (Hunter *et al*., 2012) and Pfam (Punta *et al*., 2012), while structurally and functionally important residues in the protein sequence were identified using ConSeq (Berezin *et al*., 2004) in ConSurf server.

Amplification and cloning of *csor*$_{Gz}$ gene

Geobacillus zalihae was cultivated in 10 mL Luria Bertani (LB) broth (MILLER) (Merck) at 60 °C, 230 rpm for 18 h. Genomic DNA was extracted using Wizard® Genomic DNA Purification Kit (Promega) based on the manufacturer’s recommendations. Amplification of *csoR*$_{Gz}$ gene was performed in a 25 µL mixture (1× Green GoTaq® Flexi Buffer, 1.5 mM $MgCl_2$, 0.2 mM dNTP mixture, 0.2 µM of each primer, 1 U of GoTaq® Flexi DNA Polymerase (Promega), 100 ng *G. zalihae* genomic DNA), with the following PCR condition: 94 °C for 2 min, followed by 30 cycles of amplification (95 °C for 30 sec, 53 °C for 30 sec, 72 °C for 18 sec) and a final extension at 72 °C for 6 min. Specially designed primers were used: 5’-GCAGCTAGCATGAGTGAAAAAAATCGTG-3’ (forward) and 5’-GGCGCTCGAGCTAAAGCTTTTTTAAATC-3’ (reverse) (underlined sequences denoting *Nhe*I and *Xho*I restriction sites flanking the 5’ and 3’ end of the amplified gene). Results were observed via 1% (w/v) agarose gel electrophoresis, and the amplicon was purified using Wizard® SV Gel and PCR Clean-Up System (Promega) following the manufacturer’s recommendations. *Nhe*I/*Xho*I double digestion in 30 µL digestion mixtures (1× FastDigestTM buffer (Thermo Scientific), 1U FastDigestTM *Nhe*I, 1 U FastDigestTM *Xho*I, 100 ng DNA) was performed on the purified amplicon and pET-28b(+) plasmid, at 37 °C for 10 min, before ligation for 18 h at 4 °C using 2U of T4 DNA ligase (Thermo Scientific). Transformation of *E. coli* TOP 10 with ligated product was performed using the heat shock method (Sambrook, 1989). Transformed cells were plated on LB agar containing 50 µg/mL kanamycin and incubated at 37 °C for 18 h. Verification of inserts was performed via colony PCR and DNA sequencing of the transformants using primers and PCR conditions mentioned above. The verified plasmid was then transformed into *E. coli* BL21 Star™ (DE3).

 ISSN (print): 1823-8262, ISSN (online): 2231-7538

Malays. J. Microbiol. Vol 20(4) 2024, pp. 417-429
DOI: http://dx.doi.org/10.21161/mjm.230265

Overexpression and purification of $CsoR_{Gz}$

To a 200 mL LB medium containing 50 µg/mL kanamycin, 2 mL of an overnight culture of *E. coli* BL21 StarTM (DE3) containing pET-28b(+):*csoR*$_{Gz}$ was added and cultivated at 37 °C, 230 rpm until its optical density at 600 nm reached 0.6. Isopropyl β-D-1-thiogalactopyranoside (IPTG) (0.1 mM) was then added, and the culture was further cultivated at 37 °C for 18 h. Subsequently, cells were harvested by centrifugation at 3220× *g* for 15 min, resuspended in 5 mL of binding Buffer A (10 mM 2-(N-morpholino) ethanesulfonic acid (MES) (pH 6.5), 500 mM NaCl and 50 mM imidazole) and were homogenized by sonication for 6 min with 30 sec on/off pulse at 40% amplitude. Crude cell extracts were obtained via centrifugation at 6100× *g*, 4 °C for 25 min, filtered using a 0.45 µm syringe filter and applied to the Ni^{2+}-NTA charged His-Trap Fast Flow (FF) column (XK 16/20). Purification of $CsoR_{Gz}$ protein was performed using 5-column volume (CV) Buffer B (10 mM MES (pH 6.5), 500 mM NaCl and 50 mM imidazole) at 1 mL/min. A second step purification by gel filtration chromatography using Superdex 200 (GE Healthcare) column using 2 CV of MES buffer (pH 6.5) (100 mM NaCl, 2 mM dithiothreitol (DTT), 2 mM ethylenediaminetetraacetic acid (EDTA) and 5% (v/v) glycerol) was performed at a flow rate of 1.2 mL/min. The protein was concentrated via ultracentrifugation at 4,025× *g* at 4 °C by using an Amicon centrifugal filter (Merck) with regenerated cellulose membrane with a cut-off size of 10.0 kDa. The concentration of protein obtained was determined through Bradford assay (Bradford, 1976) by using The Quick Start™ Bradford reagent (Bio-Rad).

Subunit and secondary structure composition analysis of $CsoR_{Gz}$

Subunit composition of $CsoR_{Gz}$ [in MES buffer (pH 6.5) (100 mM NaCl, 2 mM dithiothreitol (DTT), 2 mM ethylenediaminetetraacetic acid (EDTA) and 5% (v/v) glycerol)] was determined via size exclusion chromatography using Superdex 75 10/300 GL column (GE Healthcare) and protein standards consisting of aprotinin (Mw = 6500, source: bovine lung), ribonuclease A (Mw = 13700, source: bovine pancreas), carbonic anhydrase (Mw = 29000, source: bovine erythrocytes) and ovalbumin (Mw = 44000, source: hen egg white). In addition, the secondary structure of $CsoR_{Gz}$ was determined via far-UV circular dichroism (CD) by using a far UV spectropolarimeter (Chirascan Plus) in a 0.1 cm quartz cell at room temperature and wavelengths of 180-260 nm with 1 nm interval. For this purpose, the purified protein solution was subjected to buffer exchange to 20 mM MOPS buffer (pH 7) through ultracentrifugation at 4,025× *g* at 4 °C by using an Amicon centrifugal filter (Merck) with regenerated cellulose membrane with cut-off size of 10.0 kDa. CD data were analyzed using DichroWeb (CONTIN and SELCON3 self-selected algorithms).

Crystallization and structure determination of $CsoR_{Gz}$

Crystallization screening was performed with 10 mg/mL purified $CsoR_{Gz}$ protein using Hampton crystal screening kit I and II, Index kit I and II, and Molecular Dimension JSCG kit I and II through sitting-drop vapour-diffusion method with 1:1 protein to crystal formulation ratio at 15 °C. A single protein crystal obtained was placed into a cryoprotectant solution (10% (w/v) polyethylene glycol monomethyl ether 5,000) containing 5% (v/v) glycerol, flash-frozen at 100 K nitrogen stream and diffracted using an in-house Rigaku X-ray diffractometer at Malaysia Genome and Vaccine Institute (MGVI) using copper wavelength at 1.54 Å with a CCD MSC PAD200sk detector at 100 K. The data collected was processed using DENZO and SCALEPACK from HKL-3000. Suitable structural template was identified using Molecular Replacement with Bulk Model Preparation (MrBUMP) (Keegan and Winn, 2008) in the Collaborative Computational Project, Number 4 (CCP4) suite (Winn *et al*., 2011). Non-conserved side chains diverged from the target sequence were pruned using CHAINSAW (Keegan *et al*., 2011) and the protein model was built using Molrep (Vagin and Teplyakov, 1997) and Crystallographic Object-Oriented Toolkit (Coot) (Emsley and Cowtan, 2004). Structural refinement was performed using REFMAC5 (Murshudov *et al*., 1997) in CCP4 suite (Winn *et al*., 2011) and subsequently validated using PROCHECK (Laskowski *et al*., 1993), ERRAT (Colovos and Yeates, 1993) and PROSESS (Berjanskii *et al*., 2010). Secondary structures and disordered regions were analyzed using PDBsum at EMBL-EBI (Laskowski *et al*., 1997); DisEMBL (Linding *et al*., 2003) and IUPred (Dosztányi *et al*., 2005), respectively, while B factor values were generated using CPP4 (Winn *et al*., 2011). The biological assembly of $CsoR_{Gz}$ was determined using Protein Interfaces, Structures, and Assemblies (PISA) (PDBe) (Krissinel and Henrick, 2007). All structural visualization was conducted using Pymol (The PyMOL molecular graphics system, Version 2.0, Schrödinger, LLC) and Yet Another Artificial Reality Application (YASARA) (Krieger *et al.*, 2002).

Biophysical characterization of $CsoR_{Gz}$ HP *in vitro* interaction between $CsoR_{Gz}$ and Cu(I)

The interaction of $CsoR_{Gz}$ with Cu(I) was investigated via UV/Vis spectroscopy and fluorescence spectroscopy based on the method adapted from Ma *et al*. (2009) with slight modification. Buffer exchange of the purified protein solution to 20 mM MOPS buffer (pH 7) was performed through ultracentrifugation at 4,025× *g* at 4 °C by using an Amicon centrifugal filter (Merck) with regenerated cellulose membrane with cut-off size of 10.0 kDa. Twenty µM of CsoR-like HP in 20 mM MOPS buffer (pH 7) was degassed and titrated with 0-1 mM Cu(I)Cl with 0.05 mM increment. With each titration, absorption data was recorded from 200-450 nm at an optical path length of 1 cm. For fluorescence spectroscopy, the emission wavelengths were scanned from 300-500 nm with each

 ISSN (print): 1823-8262, ISSN (online): 2231-7538

Malays. J. Microbiol. Vol 20(4) 2024, pp. 417-429
DOI: http://dx.doi.org/10.21161/mjm.230265

Table 1: Top 10 PSI-BLAST results for $CsoR_{Gz}$-like HP against NR database.

Hits	Query coverage (%)	E-value	Maximum identity (%)	Accession number
MULTISPECIES: metal-sensing transcriptional repressor [*Geobacillus*]	98	1e-61	100.00	WP_020754474.1
Metal-sensing transcriptional repressor [*Bacillus* sp. HMSC76G11]	92	3e-46	81.82	WP_070878596.1
Metal-sensing transcriptional repressor [*Sporosarcina globispoara*]	87	5e-44	84.34	WP_053435904.1
Metal-sensing transcriptional repressor [*Bacillus* sp. YR335]	87	2e-43	83.13	WP_111617976.1
Metal-sensing transcriptional repressor [*Aeribacillus pallidus*]	82	8e-43	88.46	WP_063386497.1
Metal-sensing transcriptional repressor [*Bacillus* sp. OV166]	90	1e-42	76.74	WP_088087378.1
Metal-sensing transcriptional repressor [*Aeribacillus composti*]	82	4e-42	87.18	WP_144596920.1
Metal-sensing transcriptional repressor [*Aeribacillus pallidus*]	82	5e-42	87.18	WP_094244935.1
Metal-sensing transcriptional repressor [*Bacillus aciditolerans*]	96	9e-42	69.57	WP_121445156.1
Metal-sensing transcriptional repressor [*Bacillus* sp. URHB0009]	90	2e-40	74.42	WP_027322955.1

Table 2: PSI-BLAST results for $CsoR_{Gz}$-like HP against PDB.

Hits	Query coverage (%)	E-value	Identity (%)	PDB ID
Chain A, crystal structure of the copper-sensing repressor Csor with Cu(I) from *Geobacillus thermodenitrificans* Ng80-2	74	7e-12	37	4M1P
Chain A, crystal structure of the apo form of a copper-sensitive operon regulator (Csor) protein from *Streptomyces lividans*	74	6e-10	38	4ADZ
Chain A, crystal structure of Cu(I) bound Csor from *Mycobacterium tuberculosis*	77	2e-07	30	2HH7
Chain A, frmr [*Salmonella enterica* subsp. enterica serovar Typhimurium]	69	2e-04	33	5LCY

titration at an excitation wavelength of λ_{ex}=280 nm. The slits were 10 nm for both emission and excitation slits.

Docking analysis of dimeric $CsoR_{Gz}$ HP-Cu(I) complex

AutoDock Vina (Trott and Olson, 2010) was used to dock two Cu(I) metal ions at both metal-binding sites of the dimeric model of $CsoR_{Gz}$ crystal structure (PDB I.D: 6AHX). Histidine residues in the structure were firstly protonated prior to docking, as recommended by (Kim *et al*., 2013), as they can be readily switched between doubly protonated cationic states to neutral states at pH 6.0. Docking grids and dimensions were set with the specific docking parameters with an exhaustiveness of 100. The grids were placed at the metal binding sites (sites 1 and 2) of the CsoR dimer within a range of 0.375 Å from the metal binding residues, i.e., Cys46, His71 and Cys75. Each simulation cell was centered separately at the two Cu(I) binding sites covering C46, H71, and C75 residues situated at the right (labelled as site 1) and left (labelled as site 2) ends of the structure. LigPlot (Wallace *et al*., 1995) was used to visualize and compare the interaction of docked molecules, and Pymol (The PyMOL molecular graphics system, Version 2.0, Schrödinger, LLC) was used to view the interactions and distances between Cu(I) and its ligands.

RESULTS AND DISCUSSION

$CsoR_{Gz}$ protein sequence analysis

With a domain belonging to the CsoR-like DUF156 superfamily of proteins, PSI-BLASTP similarity analysis on $CsoR_{Gz}$ revealed that it had 82-100 percent similarity with a majority of HPs from various organisms (Table 1). According to InterPro and Pfam analyses, $CsoR_{Gz}$ is a member of the metal-sensitive transcriptional repressor protein family, which is involved in resistance to metal ions such as copper, nickel, and cobalt. A search against PDB gave forth three hits with low structural identity to

 ISSN (print): 1823-8262, ISSN (online): 2231-7538

Malays. J. Microbiol. Vol 20(4) 2024, pp. 417-429
DOI: http://dx.doi.org/10.21161/mjm.230265

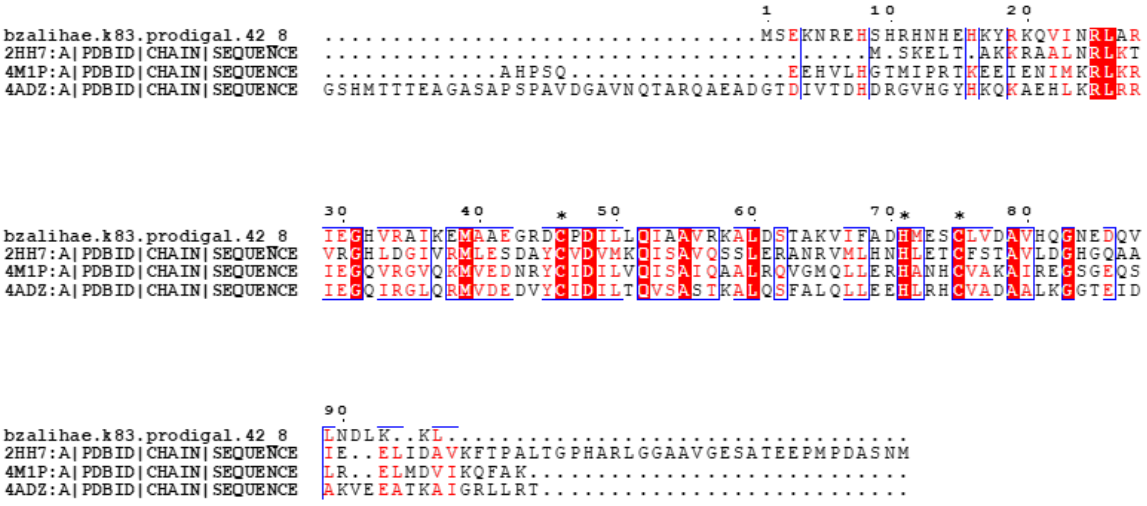

Figure 1: Multiple sequence alignment of $CsoR_{Gz}$-like HP with Csor proteins from *G. thermodenitrificans* Ng80-2 (4M1P), *S. lividans* (4ADZ) and *M. tuberculosis* (2HH7). Fully conserved residues are shown in red boxes. Residues with asterisks (*) are residues for copper binding, which form the C-H-C copper-binding motif. Similar residues in a group and across groups are represented by red letters and blue frames, respectively. Numbers above the sequences refer to amino acid numbers.

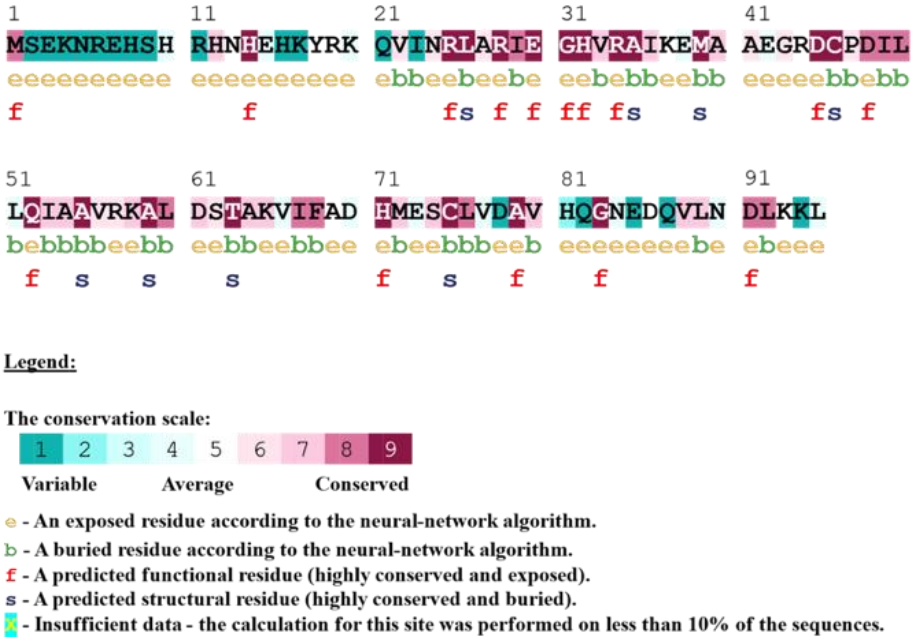

Figure 2: ConSeq result for CsoRGz-like HP.

$CsoR_{Gz}$, namely, CsoR proteins from *G. thermodenitrificans* Ng80-2, *S. lividans* and *M. tuberculosis* (PDB I.D.: 4M1P, 4ADZ and 2HH7 respectively) (Table 2). Multiple sequence alignment results revealed several well-conserved residues, including the Cys-His-Cys motif (corresponding to Cys46, His71 and Cys75 in $CsoR_{Gz}$) (Figure 1). ConSeq analysis predicted that 15 residues in the protein sequence are highly conserved, exposed and functionally important, i.e., Met1, His14, Arg25, Arg28, Glu30, Gly31, His32, Arg34, Asp45, Asp48, Gln52, His71, Ala79, Gly83 and Asp91; and 8 highly conserved and buried residues were predicted to be structurally important, i.e., Leu26, Ala35, Met39, Cys46, Ala55, Ala59, Thr63 and Cys75) (Figure 2). The presence of the conserved Cys46-His71-Cys75 motif in $CsoR_{Gz}$ highlights their involvement in Cu(I) binding. Cysteine and histidine are well-known, common amino acids that usually act as metal-binding ligands.

 ISSN (print): 1823-8262, ISSN (online): 2231-7538

Malays. J. Microbiol. Vol 20(4) 2024, pp. 417-429
DOI: http://dx.doi.org/10.21161/mjm.230265

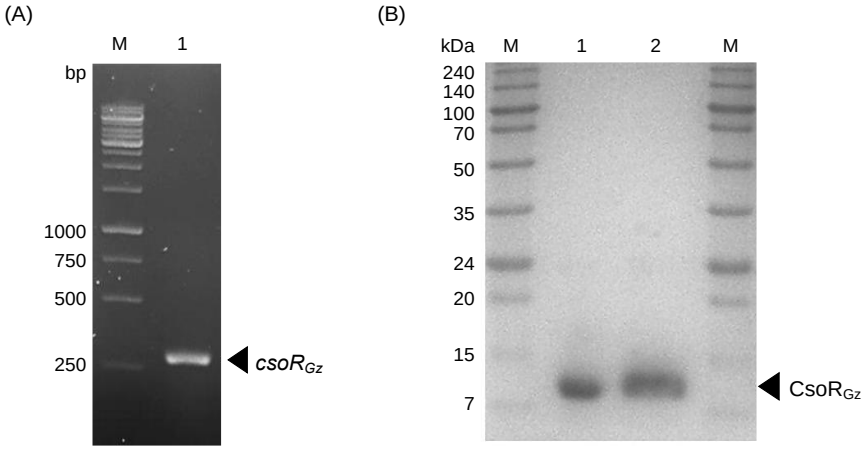

Figure 3: (A) *csoR*$_{Gz}$-like HP open-reading-frame (Lane 1, as indicated by black triangular arrow) amplified from genomic DNA of *G. zalihae*. Lane M refers to 1 kbp ladder (Thermo Scientific) with size range of 250 to 10000 bp; (B) SDS-PAGE analysis of purified CsoR$_{Gz}$-like HP. Lane M: BLUelf pre-stained protein ladder (GeneDirex) with a size range of 3.5-245 kDa, Lane 1 and 2: Purified CsoR$_{Gz}$ protein (as indicated by black triangular arrow).

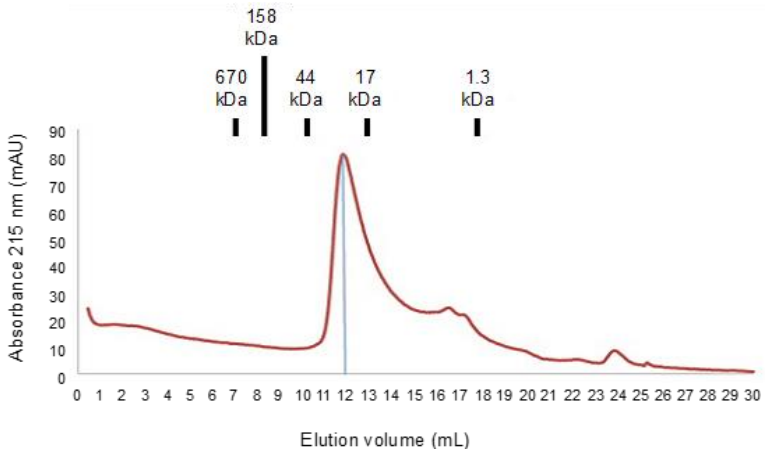

Figure 4: Chromatographic separation of CsoR$_{Gz}$-like protein sample via size exclusion chromatography using Superdex 75 10/300 GL column.

Cysteine can play a structural role excellently by binding to metals with its sulfhydryl side chain, whilst histidine can play a functional role via its neutral or positively charged side chain (Betts and Russell, 2003).

Subunit and secondary structure composition of CsoR$_{Gz}$

csoR$_{Gz}$ gene was amplified from the genomic DNA of *G. zalihae* via PCR (Figure 3A) and its optimal expression was achieved at 37 °C after 18 h of cultivation upon induction with 0.1 mM IPTG. The protein was purified to homogeneity (Figure 3B). Size exclusion chromatography analysis of CsoR$_{Gz}$ showed a single distinct peak corresponding to 29.6 kDa (Figure 4), resembling the approximate size of the protein dimer. Dynamic light scattering revealed that CsoR$_{Gz}$ has a hydrodynamic diameter of 5.0 ± 1.8 nm, while CD data showed that it is composed mainly of helices (82.3%), followed by beta-turns (9.8%), random coils (5.8%), parallel beta sheets (1.7%) and antiparallel beta sheets (0.7%) (Figure 5). This is comparable to the main secondary structure components of CsoR proteins from *G. thermodenitrificans* Ng80-2 (PDB I.D.: 4M1P), *S. lividans* PDB I.D.: 4ADZ) and *M. tuberculosis* (PDB I.D.: 2HH7) (Table 2) with helices constituting 75.3-89.0%, turns constituting 3.9-12.9% and random coils constituting 7.2-13.6%.

Analyses of CsoR$_{Gz}$ crystal structure

Single protein crystals formed in reservoir containing 5% (v/v) tacsimate TM pH 7.0, 0.1 M HEPES pH 7.0, 10% (w/v) PEG monomethyl ether 5000 were diffracted at 1.54 Å with space group of P3121 (Table 3). CsoR Chain C of *Thermus thermophilus* HB8 (PDB code: 3AAI) was identified as the appropriate structural template using

 ISSN (print): 1823-8262, ISSN (online): 2231-7538

Malays. J. Microbiol. Vol 20(4) 2024, pp. 417-429
DOI: http://dx.doi.org/10.21161/mjm.230265

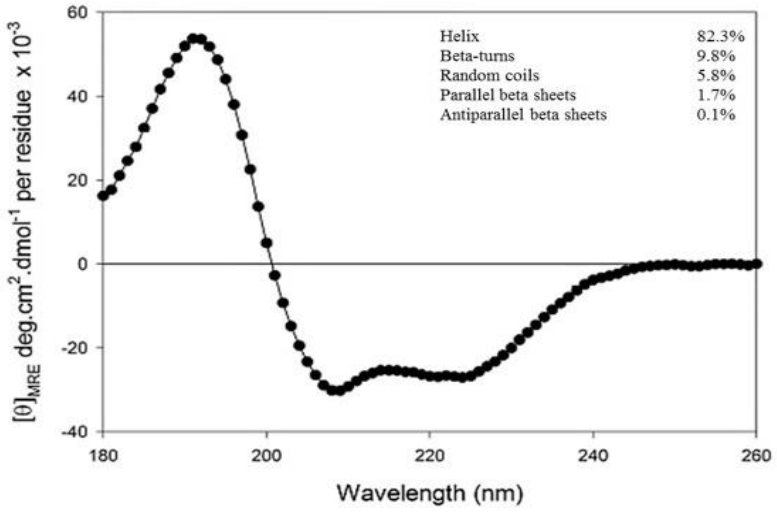

Figure 5: Far-UV CD spectrum of purified CsoRGz-like protein.

Table 3: $CsoR_{Gz}$ HP X-ray crystallographic data and statistics.

Data collection statistics	
Data collection site	MGVI in-house X-ray diffractometer (Rigaku micromax 007 hf)
Detector	CCD MSC PAD200sk
Wavelength (Å)	1.5418
Space group	P 3_1 2 1
Data resolution (Å)	40.00-2.00 (2.07-2.00)
Total number of reflections	38791
Number of unique reflections	6528 (666)
Multiplicity	5.80 (4.00)
Completeness (%)	97.40 (100.00)
R_{merge}	0.031 (0.028)
$\langle I/\sigma(I) \rangle$	45.70 (4.35)
Unit cell dimensions	
(*a, b, c*) (Å)	44.73, 44.73, 82.37
(α, β, γ) (°)	90, 90, 120
Refinement	
Resolution range (Å)	38.74-2.00 (2.03-2.00)
No: residues/water	60/48
R_{work}	0.198 (0.200)
R_{free}	0.257 (0.280)
Rms bond length deviation (Å)	0.018
Rms bond angle deviation (°)	1.98
Ramachandran angles (Favored/allowed/ disallowed) (%)	100.00/0.00/0.00

MrBUMP. Despite the fact that 3AAI did not appear in the PSI-BLAST PDB search (Table 2), pairwise alignment of its sequence with $CsoR_{Gz}$ revealed they have similar lengths and share higher sequence conservation (Figure 6) than other counterparts in Figure 1. MrBUMP was used to score the structural template and the best final refinement R_{free} score of 0.257 was achieved. Assessments of $CsoR_{Gz}$ protein crystal structure (PDB I.D: 6AHX) via Ramachandran plot analysis showed that 100% of its residues are located in the most favored regions (Table 3), while ERRAT gave forth 100% average overall quality factor. In addition, Global Structure Assessment by PROSESS revealed that covalent and non-covalent bonds, as well as torsion angles in the $CsoR_{Gz}$ protein crystal structure, are of good quality. The results of these analyses highlight that $CsoR_{Gz}$ protein crystal structure is of good quality and acceptable. The crystal structure of $CsoR_{Gz}$ protein (PDB I.D: 6AHX) revealed that it is composed of three alpha helices. The three Cu(I) binding residues can be observed in the crystal structure, namely Cys46 at the α2 helix region, His71 at the small loop located between α2 and α3 and

 ISSN (print): 1823-8262, ISSN (online): 2231-7538

Malays. J. Microbiol. Vol 20(4) 2024, pp. 417-429
DOI: http://dx.doi.org/10.21161/mjm.230265

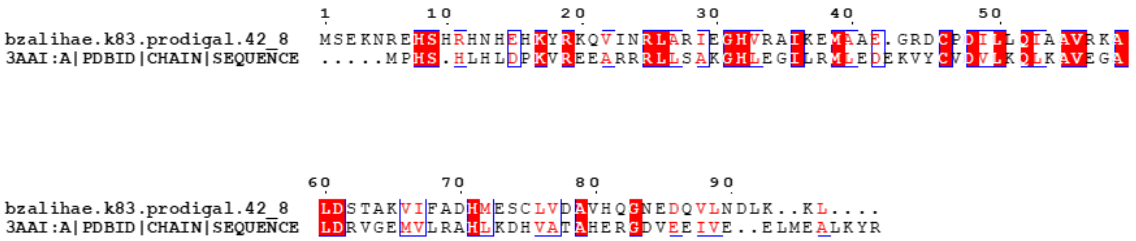

Figure 6: Pairwise alignment of $CsoR_{Gz}$-like HP with CsoR from *T. thermophilus* HB8 (PDB code: 3AAI). Fully conserved residues are shown in red boxes. Similar residues in a group and across groups are represented by red letters and blue frames, respectively. Numbers above the sequences refer to amino acid numbers.

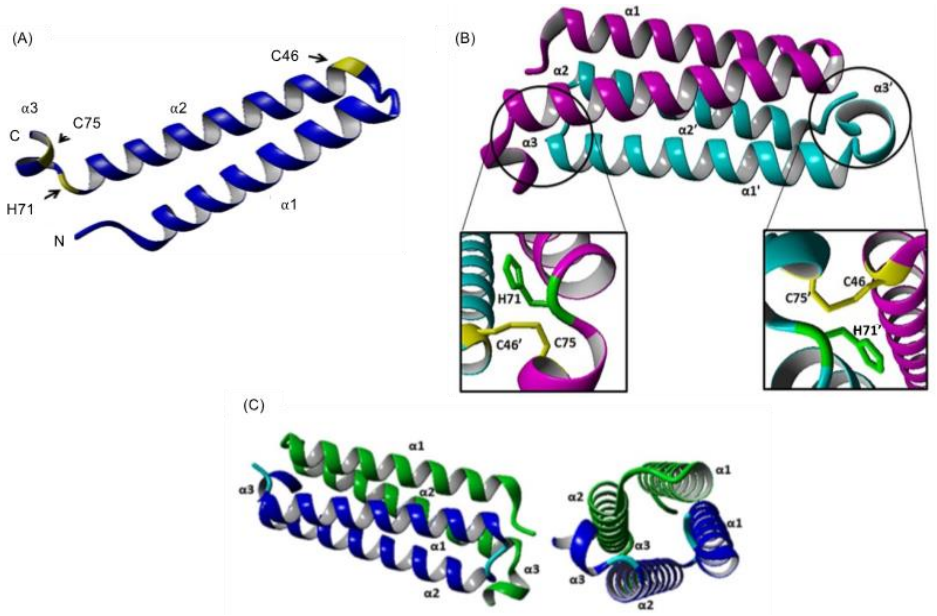

Figure 7: Overall crystal structure of (A) $CsoR_{Gz}$ containing one molecule in an asymmetric unit and dimeric structure of $CsoR_{Gz}$ protein; (B) close-up view of the two Cu(I) binding sites where site 1 (C46'-H71-C75) and site 2 (C46-H71'-C75') are located at both the ends of the dimeric structure and (C) side and front view (PDB ID: 6AHX).

Cys75 at the short α3 helix (Figure 7A). The small loop (or 'helix hairpin') connects three antiparallel alpha helices. At both the N- and C-terminals, DisEMBL and IUPred data revealed disorder and flexibility (high B factor value) (Figure 8).

Symmetry analysis of the density map of $CsoR_{Gz}$ indicated that symmetry-related residues are present at both active sites, with Cys46 interacting with the symmetric residue Cys75' and Cys75 residue interacting with the symmetric residue Cys46' (Figure 7B). $CsoR_{Gz}$ has a biological interface and exists as a homodimer (Figure 7B and 7C) with a buried interface of 1367.5 Å, according to PISA results (Table 4).

These findings further suggest that the biological assembly of $CsoR_{Gz}$ protein is dimeric. Although it only comprises one subunit in its asymmetric unit composition (Table 4), this does not necessarily reflect the entire biological ensemble of multimeric proteins (Betts and Russell, 2003). The monomers in the dimeric structure of $CsoR_{Gz}$ were stabilized by two disulphide bonds (in the absence of Cu(I)), salt bridges, hydrogen bonds and mainly hydrophobic interactions (Figure 7B, Figure 9A and Table 5). Other than that, α1 and α2 are packed against α1' and α2' from the symmetry-related protomer in the dimer, with C46 situated on the loop connecting α1 and α2 and H71 and C75 located at the end of α2. This geometry is similar to those found in CsoR structures of *S. lividans* (Dwarakanath *et al*., 2012) and *M. tuberculosis* (Liu *et al*., 2007).

It is interesting to note that albeit displaying low sequence identity to other reported CsoR proteins, the crystal structure of $CsoR_{Gz}$ showed structural similarity to well-characterized CsoRs from *G. thermodenitrificans* Ng80-2 (Chang *et al*., 2014), *M. tuberculosis* (Liu *et al*., 2007), *S. lividans* (Dwarakanath *et al*., 2012) and *T. thermophilus* (Sakamoto *et al*., 2010), which mainly consisted of helices and coils. In addition, the dimeric nature of $CsoR_{Gz}$ is in agreement with the homodimeric

 ISSN (print): 1823-8262, ISSN (online): 2231-7538

Malays. J. Microbiol. Vol 20(4) 2024, pp. 417-429
DOI: http://dx.doi.org/10.21161/mjm.230265

Table 4: Assembly summary for the dimeric structure of $CsoR_{Gz}$ protein generated by PISA.

Assembly summary	
Multimeric state	2
Copies in a unit cell	3
Formula/Composition	A2
Dissociation pattern	2(A)
Surface area (Å^2)	6714.1
Buried area (Å^2)	2735.0
Interface area (Å^2)	4724.5
ΔGint (kcal/mol)	-28.5
ΔGdiss (kcal/mol)	31.1
TΔSdiss (kcal/mol)	10.7
Symmetry	2

Table 5: Key residues and interactions involved in stabilizing dimeric $CsoR_{Gz}$ structure.

Residues	Interactions
Lys37'-Glu30	Salt bridges
Lys37-Glu30'	
Glu37'-Arg34	
Glu37-Arg34'	
Lys37'-Glu30	Hydrogen bonds
Lys37-Glu30'	
Arg34'-Glu30	
Arg34-Glu30'	
Tyr18'-Arg44	
Tyr18-Arg44'	
Cys46'-Cys75	
Cys46-Cys75'	
Arg57'-Arg57	
Arg57-Arg57'	
Tyr18'-Ile49	Hydrophobic interaction
Tyr18-Ile49'	
Ala41'-Ile23	
Ala41-Ile23'	
Ile67'-Ile49	
Ile67-Ile49'	
Ala64'-Ile53	
Ala64-Ile53'	
Leu50'-Ile67	
Leu50-Ile67'	
Leu60'-Val33	
Leu60-Val33'	
Arg57'-Arg57	
Arg57-Arg57'	
Leu26'-Ile53	
Leu26-Ile53'	
Ala27'-Lys37	
Ala27-Lys37'	
Glu30'-Val33	
Glu30-Val33'	
Ala40'-Ile23	
Ala40-Ile23'	
Gly43'-Tyr18	
Gly43-Tyr18'	
Phe68'-Leu50	
Phe68-Leu50'	

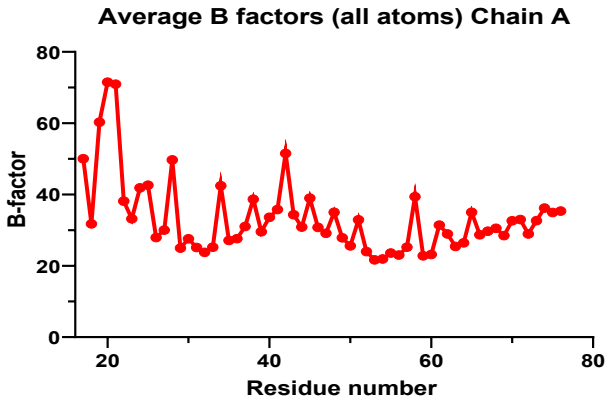

Figure 8: B-factor profile of CsoRGz crystal structure with the average B-factor value of 34.

and homotetramic forms reported for CsoRs of *M. tuberculosis* (Liu *et al*., 2007), *T. thermophilus* and *S. lividans* (Sakamoto *et al*., 2010; Dwarakanath *et al*., 2012), respectively.

Biophysical characterization of $CsoR_{Gz}$ HP

When $CsoR_{Gz}$ was titrated with 0-1 mM Cu(I)Cl, UV/Vis spectroscopy revealed an increase in absorbance at 240 nm and a decrease in fluorescence intensity at 280 nm through fluorescence spectroscopy (Figure 10A and 10B). Complex formation and oxidation of the thiol group (Rigo *et al*., 2004) eventually led to the electronic transition of the molecules depicted by the increase in absorbance at 240 nm via UV/Vis spectrophotometry (Liu *et al*., 2008; Upstone, 2013). Such observation is similar to those reported in other studies of CsoR proteins (Liu *et al*., 2007; Ma *et al*., 2009; Dwarakanath *et al*., 2012). Besides UV/Vis spectrophotometry, fluorescence spectroscopy is a sensitive technique used to monitor the biochemical environment of a fluorophore. The fluorophores in proteins are primarily tyrosine and tryptophan amino acids, with aromatic rings in their side chains serving as the components that emit fluorescence (So and Dong, 2001). The decrease in intensity observed through fluorescence spectroscopy indicates an interaction between the $CsoR_{Gz}$ and Cu(I), complementing the results obtained via UV/Vis. These results suggest an interaction between $CsoR_{Gz}$ and Cu(I).

Docking analysis of dimeric $CsoR_{Gz}$-Cu(I) complex

The possibility of Cys46, Cys75 and His71 to coordinate Cu(I) metal ions was demonstrated in docking investigations of Cu(I) to the crystal structure of $CsoR_{Gz}$. Docking in both binding pockets showed that the protein was able to interact with Cu(I) (Figure 9B), with a binding energy of -0.8 kcal/mol. In addition to this, dimerization of CsoR proteins has been reported to be essential for Cu(I)-binding (Tan *et al*., 2014), which is aided by the presence of the Cys-His-Cys Cu(I)-binding ligands in α2. This can be similarly observed in $CsoR_{Gz}$, where Cys46-

 ISSN (print): 1823-8262, ISSN (online): 2231-7538

Malays. J. Microbiol. Vol 20(4) 2024, pp. 417-429
DOI: http://dx.doi.org/10.21161/mjm.230265

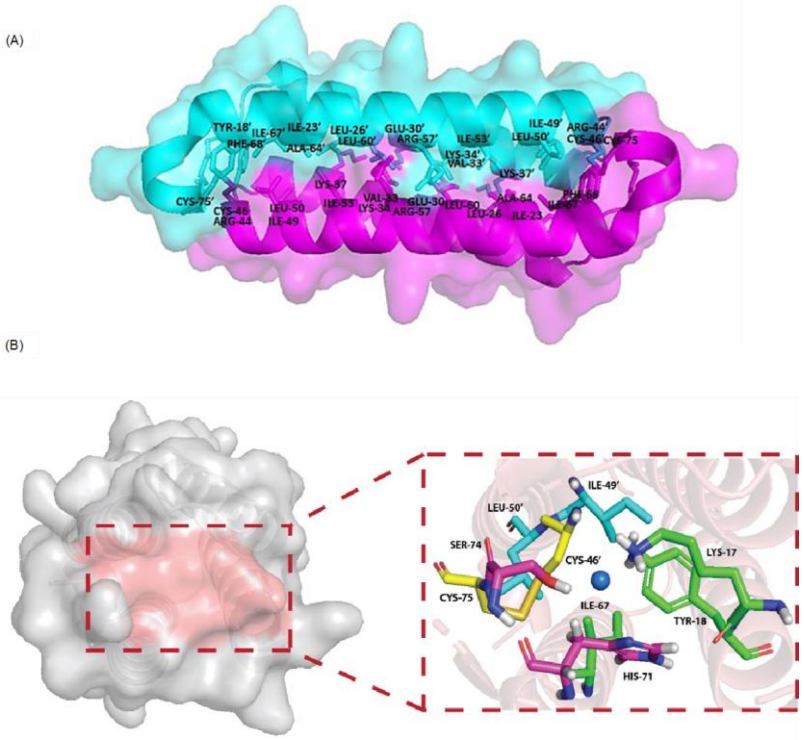

Figure 9: (A) Amino acid residues involved in the stabilization of the dimeric structure of $CsoR_{Gz}$ protein by forming hydrogen bonds, disulphide bonds, salt bridges and hydrophobic interactions connecting the monomers. (B) Close-up view of amino acid residues involved in providing a hydrophobic environment in the Cu(I) binding site of $CsoR_{Gz}$ within 5 Å radius from the metal binding site.

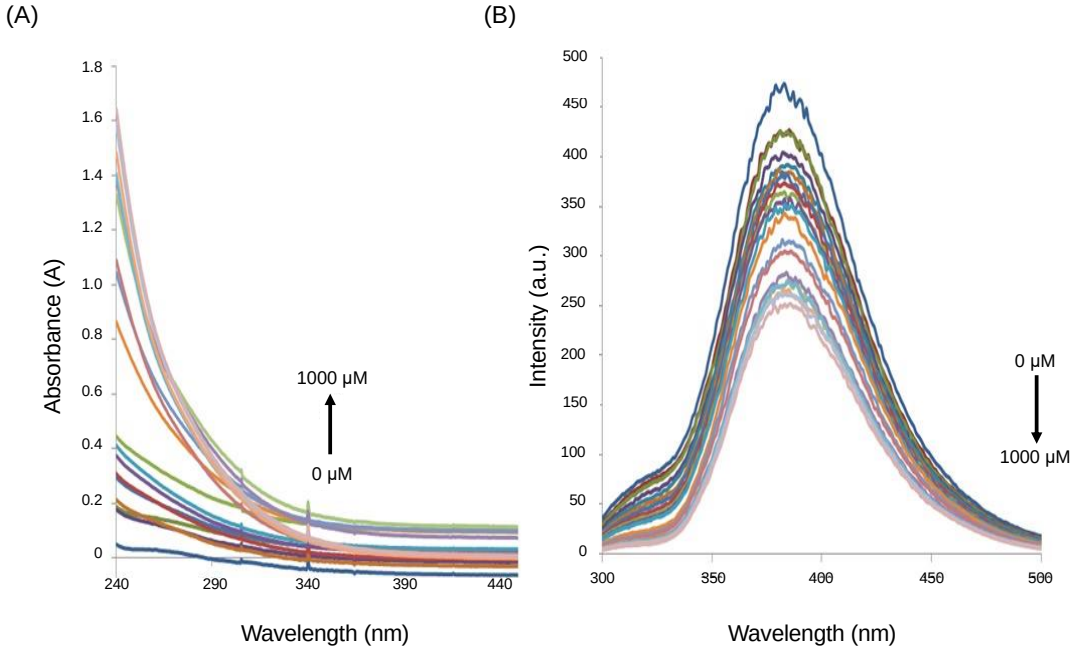

Figure 10: (A) Gradual increase in 240 nm absorption with titration of 0-1 mM Cu(I)Cl (with 0.05 mM increment) to 20 µM of $CsoR_{Gz}$-like HP in 20 mM MOPS buffer (pH 7); (B) Decreased in fluorescence intensity with titration of 0-1 mM Cu(I)Cl (with 0.05 mM increment) to 20 µM of $CsoR_{Gz}$-like HP in 20 mM MOPS buffer (pH 7).

 ISSN (print): 1823-8262, ISSN (online): 2231-7538

Malays. J. Microbiol. Vol 20(4) 2024, pp. 417-429
DOI: http://dx.doi.org/10.21161/mjm.230265

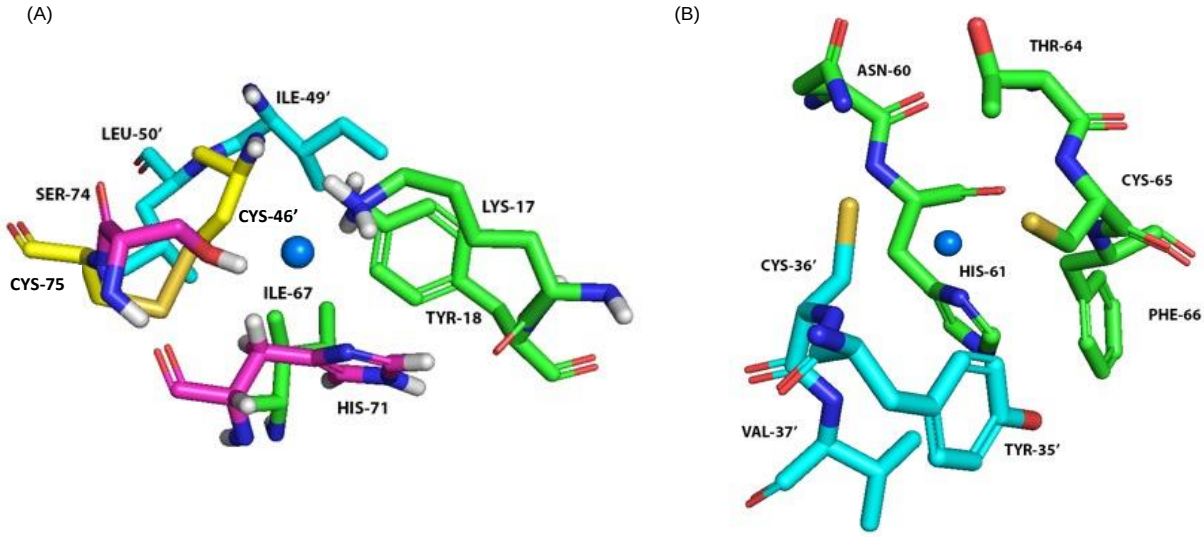

Figure 11: Comparison of Cu(I) binding site of (A) $CsoR_{Gz}$ (PDB ID: 6AHX) and (B) *Mtb* CsoR (PDB ID: 2HH7).

His71-Cys75 was also found to be located on α2. In addition to α2, interactions between α3 helices in the dimers are important in maintaining the dimeric assembly of CsoR protein (Tan *et al*., 2014). Two of the metal-binding ligands (Cys and His) are located at the C-terminal end of α2, while the second Cys residue is located at the N-terminal end of α2' in the protein dimer (Tan *et al*., 2014). In this form, two Cu(I) ions will bind to the CsoR dimer. One Cu(I) ion will be coordinated by Cys and His from one monomer, and the second Cu(I) ion will be coordinated by Cys at the other monomer, similar to other reported CsoR proteins (Liu *et al*., 2007; Dwarakanath *et al*., 2012). This will form a trigonal inter-subunit binding complex (trigonal planar coordination) between the Cys thiolate and Nδ2 of the His residue and Cu(I) (Tan *et al*., 2014). It was reported that residues 12 to 19 at the N-terminal of Cu(I)-bound *Gt* CsoR formed interactions with Cu(I), resulting in the formation of a kink at the α2 regions (Chang *et al*., 2014). Similarly, in $CsoR_{Gz}$, Lys17 and Tyr18 at the N-terminal end of α2 were found to be interacting with Cu(I) (Figure 9B and 11A). In *Mtb* CsoR, Lys8, Lys15, Arg52, Arg55, His59, Cys36, Cys65', His61', Tyr35 and Glu81' formed a positively charged environment around Cu(I) binding site (Liu *et al*., 2007) (Figure 11B). Similarly, in Cu(I)-bound *Gt* CsoR, positively charged residues i.e., Arg18, Arg74, Ile16, Cys79, His75, Glu95, His12, Tyr49', Arg48', Pro17, Cys50', Glu22 were clustered around the Cu(I) binding site. These residues were reported to be responsible for conformational changes at the Cu(I) binding site upon their interaction with the metal ion from their free state (Dwarakanath *et al*., 2012). However, in $CsoR_{Gz}$, its Cu(I) binding site was surrounded by a hydrophobic environment constituted by residues Lys17, Tyr18, Cys46, Ile49, Leu50, Ile67, His71, Ser74 and Cys75 in the binding pocket (Figure 11A) and Lys17 and Tyr18 at the N-terminal end of α2 helix (Figure 9B).

CONCLUSION

In this work, $CsoR_{Gz}$-like protein was identified from the genome of a locally isolated *G. zalihae* strain T1 thermophile. Despite its relatively low sequence and structural homology to other well-characterized CsoR proteins, $CsoR_{Gz}$ contained key similarities in its metal-binding motif and structural features to its well-characterized counterparts. Further characterization of its possibly various metal-binding ability and thermal tolerance may give better insight into the properties of this protein.

ACKNOWLEDGEMENTS

This study was funded by Universiti Putra Malaysia's Postgraduate Putra Grant Scheme (GP-IPS/2016/9502200). NM and AM were funded under Universiti Putra Malaysia Graduate Research Fellowship (UPM GRF) and Ministry of Higher Education, Malaysia, MyMaster fellowships.

REFERENCES

Altschul, S. F., Gish, W., Miller, W., Myers, E. W. and Lipman, D. J. (1990). Basic local alignment search tool. *Journal of Molecular Biology* **215(3), 403-410.**

Betts, M. J. and Russell, R. B. (2003). Amino acid properties and consequences of substitutions. *In*: Bioinformatics for Geneticists. Barnes, M. R. and Gray, I. C. (eds.). John Wiley & Sons, Ltd, United Kingdom**. pp. 289-316.**

Berezin, C., Glaser, F., Rosenberg, J., Paz, I., Pupko, T., Fariselli, P. *et al.* (2004). ConSeq: The identification of functionally and structurally important residues in protein sequences. *Bioinformatics* **20(8), 1322-1324.**

 ISSN (print): 1823-8262, ISSN (online): 2231-7538

Berjanskii, M., Liang, Y., Zhou, J., Tang, P., Stothard, P., Zhou, Y. *et al.* (2010). PROSESS: A protein structure evaluation suite and server. *Nucleic Acids Research* **38(Suppl 2), W633-W640.**

Berman, H. M., Westbrook, J., Feng, Z., Gilliland, G., Bhat, T. N., Weissig, H. *et al.* (2000). The protein data bank. *Nucleic Acids Research* **28(1), 235-242.**

Bork, P. (2000). Powers and pitfalls in sequence analysis: The 70% hurdle. *Genome Research* **10(4), 398-400.**

Bradford, M. M. (1976). A rapid and sensitive method for the quantitation of microgram quantities of protein utilizing the principle of protein-dye binding. *Analytical Biochemistry* **172(1-2), 248-254.**

Chang, F. J., Coyne, H. J., Cubillas, C., Vinuesa, P., Fang, X., Ma, Z. *et al.* (2014). Cu(I)-mediated allosteric switching in a copper-sensing operon repressor (CsoR). *Journal of Biological Chemistry* **289(27), 19204-19217.**

Colovos, C. and Yeates, T. O. (1993). Verification of protein structures: Patterns of nonbonded atomic interactions. *Protein Science* **2(9), 1511-1519.**

Dosztányi, Z., Csizmok, V., Tompa, P. and Simon, I. (2005). IUPred: Web server for the prediction of intrinsically unstructured regions of proteins based on estimated energy content. *Bioinformatics* **21(16), 3433-3434.**

Dwarakanath, S., Chaplin, A. K., Hough, M. A., Rigali, S., Vijgenboom, E. and Worrall, J. A. R. (2012). Response to copper stress in *Streptomyces lividans* extends beyond genes under direct control of a copper-sensitive operon repressor protein (CsoR). *Journal of Biological Chemistry* **287(21), 17833-17847.**

Emsley, P. and Cowtan, K. (2004). Coot: Model-building tools for molecular graphics. *Acta Crystallographica. Section D, Biological Crystallography* **60(12), 2126-2132.**

Hanson, A. D., Pribat, A., Waller, J. C. and de Crécy-Lagard, V. (2009). "Unknown" proteins and "orphan" enzymes: The missing half of the engineering parts list--and how to find it. *Biochemical Journal* **425(1), 1-11.**

Hiniker, A., Collet, J. and Bardwell, J. C. A. (2005). Copper stress causes an *in vivo* requirement for the *Escherichia coli* disulfide isomerase DsbC. *Journal of Biological Chemistry* **280(40), 33785-33791.**

Hunter, S., Jones, P., Mitchell, A., Apweiler, R., Attwood, T. K., Bateman, A. *et al.* (2012). InterPro in 2011: New developments in the family and domain prediction database. *Nucleic Acids Research* **40(D1), D306-D312.**

Iwig, J. S., Rowe, J. L. and Chivers, P. T. (2006). Nickel homeostasis in *Escherichia coli* - the *rcnR-rcnA* efflux pathway and its linkage to NikR function. *Molecular Microbiology* **62(1), 252-262.**

Keegan, R. M. and Winn, M. D. (2008). MrBUMP: An automated pipeline for molecular replacement. *Acta Crystallographica. Section D, Biological Crystallography* **64(1), 119-124.**

Keegan, R. M., Long, F., Fazio, V. J., Winn, M. D., Murshudov, G. N. and Vagin, A. A. (2011). Evaluating the solution from *MrBUMP* and *BALBES*. *Acta Crystallographica. Section D, Biological Crystallography* **67(4), 313-323.**

Kim, M. O., Nichols, S. E., Wang, Y. and McCammon, J. A. (2013). Effects of histidine protonation and rotameric states on virtual screening of *M. tuberculosis* RmlC. *Journal of Computer-Aided Molecular Design* **27(3), 235-246.**

Krieger, E., Koraimann, G. and Vriend, G. (2002). Increasing the precision of comparative models with YASARA NOVA -- A self-parameterizing force field. *Proteins* **47(3), 393-402.**

Krissinel, E. and Henrick, K. (2007). Inference of macromolecular assemblies from crystalline state. *Journal of Molecular Biology* **372(3), 774-797.**

Larkin, M. A., Blackshields, G., Brown, N. P., Chenna, R., McGettigan, P. A., McWilliam, H. *et al.* (2007). Clustal W and Clustal X version 2.0. *Bioinformatics* **23(21), 2947-2948.**

Laskowski, R. A., Hutchinson, E. G., Michie, A. D., Wallace, A. C., Jones, M. L. and Thornton, J. M. (1997). PDBsum: A web-based database of summaries and analyses of all PDB structures. *Trends in Biochemical Sciences* **22(12), 488-490.**

Laskowski, R. A., MacArthur, M. W., Moss, D. S. and Thornton, J. M. (1993). PROCHECK: A program to check the stereochemical quality of protein structures. *Journal of Applied Crystallography* **26(2), 283-291.**

Linding, R., Jensen, L. J., Diella, F., Bork, P., Gibson, T. J. and Russell, R. B. (2003). Protein disorder prediction: Implications for structural proteomics. *Structure* **11(11): 1453-1459.**

Liu, T., Chen, X., Ma, Z., Shokes, J., Hemmingsen, L., Scott, R. A. *et al.* (2008). A Cu^{I}-sensing ArsR family metal sensor protein with a relaxed metal selectivity profile. *Biochemistry* **47(40), 10564-10575.**

Liu, T., Ramesh, A., Ma, Z., Ward, S. K., Zhang, L., George, G. N. *et al.* (2007). CsoR is a novel *Mycobacterium tuberculosis* copper-sensing transcriptional regulator. *Nature Chemical Biology* **3(1), 60-68.**

Ma, Z., Cowart, D. M., Scott, R. A. and Giedroc, D. P. (2009). Molecular insights into the metal selectivity of the copper(i)-sensing repressor CsoR from *Bacillus subtilis*. *Biochemistry* **48(15), 3325-3334.**

Macomber, L. and Imlay, J. A. (2009). The iron-sulfur clusters of dehydratases are primary intracellular targets of copper toxicity. *Proceedings of the National Academy of Sciences of the United States of America* **106(20), 8344-8349.**

Marchler-Bauer, A. and Bryant, S. H. (2004). CD-Search: Protein domain annotations on the fly. *Nucleic Acids Research* **32, W327-W331.**

Murshudov, G. N., Vagin, A. A. and Dodson, E. J. (1997). Refinement of macromolecular structures by the maximum-likelihood method. *Acta Crystallographica. Section D. Biological Crystallography* **53(3), 240-255.**

Punta, M., Coggill, P. C., Eberhardt, R. Y., Mistry, J., Tate, J., Boursnell, C. *et al.* (2012). The Pfam protein families database. *Nucleic Acids Research* **40(D1), D290-D301.**

Rademacher, C. and Masepohl, B. (2012). Copper-responsive gene regulation in bacteria. *Microbiology* **158(10), 2451-2464.**

Rahman, R. N. Z. R. A., Leow, T. C., Salleh, A. B. and Basri, M. (2007). *Geobacillus zalihae* sp. nov., a thermophilic lipolytic bacterium isolated from palm oil mill effluent in Malaysia. *BMC Microbiology* **7, 77.**

Rigo, A., Corazza, A., di Paolo, M. L., Rossetto, M., Ugolini, R. and Scarpa, M. (2004). Interaction of copper with cysteine: Stability of cuprous complexes and catalytic role of cupric ions in anaerobic thiol oxidation. *Journal of Inorganic Biochemistry* **98(9), 1495-1501.**

Roberts, R. J. (2004). Identifying protein function -- A call for community action. *PLoS Biology* **2(3), E42.**

Sakamoto, K., Agari, Y., Agari, K., Kuramitsu, S. and Shinkai, A. (2010). Structural and functional characterization of the transcriptional repressor CsoR from Thermus thermophilus HB8. *Microbiology* **156(7), 1993-2005.**

Sambrook, J. (1989). Molecular Cloning: A Laboratory Manual, Edn. 2nd. Cold Spring Harbor Laboratory Press, New York.

Smaldone, G. T. and Helmann, J. D. (2007). CsoR regulates the copper efflux operon *copZA* in *Bacillus subtilis*. *Microbiology* **153(12), 4123-4128.**

So, P. T. C. and Dong, C. Y. (2001). Fluorescence spectrophotometry. *In*: Encyclopedia of Life Sciences. John Wiley & Sons, Ltd, United Kingdom. pp**. 426-469.**

Tan, B. G., Vijgenboom, E. and Worrall, J. A. R. (2014). Conformational and thermodynamic hallmarks of DNA operator site specificity in the copper sensitive operon repressor from *Streptomyces lividans*. *Nucleic Acids Research* **42(2), 1326-1340.**

Trott, O. and Olson, A. J. (2010). AutoDock Vina: Improving the speed and accuracy of docking with a new scoring function, efficient optimization, and multithreading. *Journal of Computational Chemistry* **31(2), 455-461.**

Upstone, S. L. (2013). Ultraviolet/visible light absorption spectrophotometry in clinical chemistry. *In*: Encyclopedia of Analytical Chemistry. Meyers, R. A. (ed.). John Wiley & Sons, Ltd, United Kingdom. **pp. 1699-1714.**

Vagin, A. and Teplyakov, A. (1997). MOLREP: An automated program for molecular replacement. *Journal of Applied Crystallography* **30(6), 1022-1025.**

Wallace, A. C., Laskowski, R. A. and Thornton, J. M. (1995). LIGPLOT: A program to generate schematic diagrams of protein-ligand interactions. *Protein Engineering, Design and Selection* **8(2), 127-134.**

Winn, M. D., Ballard, C. C., Cowtan, K. D., Dodson, E. J., Emsley, P., Evans, P. R. *et al.* (2011). Overview of the CCP4 suite and current developments. *Acta Crystallographica D Biological Crystallography* **67(4), 235-242.**

 ISSN (print): 1823-8262, ISSN (online): 2231-7538